Available online at www.sciencedirect.com
ScienceDirect
Journal of Solid State Chemistry 180 (2007) 3571–3575
JOURNAL OF SOLID STATE CHEMISTRY
www.elsevier.com/locate/jssc

A manganese sulfite with extended metal–oxygen–metal bonds exhibiting hydrogen uptake

K. Prabhakara Rao, A. Govindaraj, C.N.R. Rao*

Chemistry and Physics of Materials Unit, CSIR Centre of Excellence in Chemistry, Jawaharlal Nehru Centre for Advanced Scientific Research, Jakkur P.O., Bangalore 560064, India

Received 31 July 2007; received in revised form 19 October 2007; accepted 22 October 2007

Abstract

A manganese sulfite of the formula $Mn_5(OH)_4(SO_3)_3 \cdot 2H_2O$, **I**{$a = 7.5759(7)$ Å, $b = 8.4749(8)$ Å, $c = 10.852(1)$ Å, $\beta = 100.732(2)^\circ$, $Z = 2$, space group $= P2_1/m$ (no. 11), $R_1 = 0.0399$ and $wR_2 = 0.1121$ [for R indexes $I > 2\sigma(I)$]}, comprising Mn_3O_{14} units and extended Mn–O–Mn bonds along the three dimensions has been synthesized under hydrothermal conditions. It has narrow channels along the b-axis and exhibits hydrogen storage of 2.1 wt% at 300 K and 134 bar.

Keywords: Manganese sulfite; Hydrothermal synthesis; X-ray diffraction; Metal–oxygen–metal bonds; Antiferromagnetism; Hydrogen storage

1. Introduction

Hybrid network and open-framework structures containing different types of anionic building units such as silicate, phosphate, sulfate and carboxylate anions, have been described adequately in the recent literature [1–11]. Some of these compounds exhibit useful adsorption properties [12–19]. Thus, a nanoporous nickel (II) phosphate exhibits hydrogen adsorption to the extent of 70 cc/g at 77 K and 1 atm, similar to many of the zeolites [12]. γ-Zirconium phosphate exhibits hydrogen adsorption of 74 cc/g at 77 K and 1 atm [13]. A microporous manganese formate is found to store hydrogen storage up to 0.9 wt% at 78 K and 1 atm [14]. In view of the importance of solid-state hydrogen storage, discovering new materials with good thermal stability and hydrogen storage properties has become a vital area of research [15–19]. Compounds capable of selective sorption of gases would also be useful in sensors and separation technology as well [20,21]. We have been interested in the design and synthesis of open-framework materials based on the sulfite ion [22]. In this effort, we have isolated a novel manganese sulfite, $Mn_5(OH)_4(SO_3)_3 \cdot 2H_2O$, **I**, with a three-dimensional structure possessing narrow one-dimensional channels, comprising Mn_3O_{14} structural units. Interestingly, this compound exhibits selective hydrogen storage going up to 2.1 wt%.

2. Experimental

2.1. Synthesis

Ammonium sulfite monohydrate, 1,4-diaminobutane and manganese (II) acetate tetrahydrate of high purity were used for the synthesis. The titled compound was synthesized by the hydrothermal method by heating the homogenized reaction mixture in a 23 mL PTFE-lined bomb at 150 °C over a period of 7 days under autogeneous pressure. The compositions of the starting mixture was as follows: $Mn(OAc)_2 \cdot 4H_2O$ (0.1245 g, 0.5 mmol), $(NH_4)_2SO_3 \cdot H_2O$ (0.1006 g, 0.75 mmol), 1,4-diaminobutane (0.03 mL, 0.25 mmol) and H_2O (5 mL, 278 mmol). The pH of the starting reaction mixture was 7 and showed little change after the reaction. The product of the hydrothermal reaction was vacuum filtered and dried under ambient conditions. The product containing colorless needle-shaped crystals was isolated in 70% yield.

*Corresponding author. Fax: +91 80 22082760, +91 80 22082766.
E-mail address: cnrrao@jncasr.ac.in (C.N.R. Rao).

0022-4596/$ - see front matter © 2007 Elsevier Inc. All rights reserved.
doi:10.1016/j.jssc.2007.10.022

2.2. Characterization

Energy dispersive analysis of X-rays (EDAX) was carried using OXFORD EDAX system. EDAX gave the expected manganese: sulfur ratio of 5:3. Infrared (IR) spectroscopic studies of KBr pellet were recorded in the mid-IR region (Bruker IFS-66v). IR spectrum of the compound showed the characteristic bands of the SO_3^{2-} ion around 970(ν_1), 620(ν_2), 930(ν_3) and 470(ν_4) cm^{-1} [23,24]. The peaks at around 3250–3500 $cm^{-1}$are attributed to OH stretching vibrations of hydroxyl group and water molecules and their bending modes are seen at around 1630 cm^{-1} [23,24]. Magnetic measurements were performed at temperatures between 2 and 300 K, in a vibrating sample magnetometer using a physical property measurement system (quantum design). Thermogravimetric analysis (TGA) was carried out (Metler–Toledo) in nitrogen atmosphere (flow rate = 50 mL/min) in the temperature range 30–900 °C (heating rate = 10 °C/min).

2.3. Gas adsorption studies

Gas adsorption experiments were performed using QUANTA CHROME AUTOSORB-1C instrument operating at 77 K (for CO_2 195 K) and 1 atm. The apparatus used for high-pressure H_2 adsorption experiments was custom-built and similar to that described elsewhere [25]. It consisted of a high-pressure stainless sample cell that was connected to high-pressure reservoir *via* a high-pressure bellow valve. The pressure was monitored using a pressure gauge that was connected in the system. Experiments were conducted to verify that the system was leak free. This was done by pressurizing the unit, and verifying that the pressure remained constant over a period of 10 h. Calibration of the system to account for the pressure drop brought about by the increase in volume upon opening of the valve between the reservoir and the evacuated sample cell at various pressures was also carried out. The volume of gas contained in the system at various pressures in the absence of the sample was determined by allowing it to exit the system and then measuring by the displacement of water. The hydrogen that was used was of ultra high purity (>99.99%), with an impurity (e.g, moisture and nitrogen) content of less than 10 ppm. The sample was accurately weighed and taken in the cell. The sample cell was evacuated to 10^{-5} Torr and heated for 5 h at 150 °C in order to degas the sample. This vacuum is sufficient as per the IUPAC recommendations on adsorption measurements [26]. Hydrogen was then introduced in to the reservoir container and subsequently let in to the sample cell. The drop in pressure from the initial value was measured at regular intervals. The amount of hydrogen stored in the samples was calculated from the changes in pressure following the interaction of the material with the gas. Blank tests were repeated at regular intervals to verify that the system was free of leaks and that the pressure drop observed was only due to the uptake of hydrogen by the sample.

2.4. X-ray diffraction and crystal structure

Powder XRD pattern of the product was recorded using Cu$K\alpha$ radiation (Rich-Seifert, 3000TT). The pattern agreed with that calculated by single crystal structure determination. A suitable single crystal was carefully selected under a polarizing microscope and glued to a thin glass fiber. Crystal structure determination was performed on a Bruker APEX II charge coupled device X-ray diffractometer equipped with a normal focus, 2.4 kW sealed tube X-ray source (Mo$K\alpha$ radiation, $\lambda = 0.71073$ Å) operating at 50 kV and 30 mA. An empirical absorption correction based on symmetry equivalent reflections was applied using the SADABS program [27]. The structure was solved and refined using the WinGX suite of programs [28]. The graphic programs DIAMOND and ORTEP were used to draw the structures [29,30]. The final refinement included atomic positions for all the atoms, anisotropic thermal parameters for all the non-hydrogen atoms and isotropic thermal parameters for the hydrogen atoms. Hydrogens of the hydroxyl group were located by difference Fourier map and included in the final refinement. Hydrogens of the water molecule were not found in the difference Fourier map and not included in the final refinement The O–H bond lengths of all the hydroxyl groups were constrained to 0.900 Å. The details of the structure solution and final refinements for **I**, are given in Table 1. Atomic coordinates of *I* are given in Table 2.

Further details of the crystal structure investigation can be obtained from the Fachinformationszentrum

Table 1
Crystal data and structure refinement parameters for **I**

Structure parameter	**I**
Empirical formula	$Mn_5S_3O_{15}H_8$
Formula weight	618.94
Crystal system	Monoclinic
Space group	$P2_1/m$ (no. 11)
a/Å	7.5759(7)
b/Å	8.4749(8)
c/Å	10.8515(11)
β/°	100.732(2)
V/Å^3	684.5(1)
Z	2
D (calc)/g/cm^3	3.003
μ/mm^{-1}	5.022
Total data collected	1062
Unique data	958
R indexes [$I>2\sigma(I)$]	$R_1 = 0.0399$[a]; w$R_2 = 0.1121$[b]
R indexes [all data]	$R_1 = 0.0430$[a]; w$R_2 = 0.1140$[b]

[a] $R_1 = \Sigma||F_0|-|F_c||/\Sigma|F_0|$.

[b] $wR_2 = \{\Sigma[w(F_0^2-F_c^2)^2]/\Sigma[w(F_0^2)^2]\}^{1/2}$. $w = 1/[\sigma^2(F_0)^2+(aP)^2+bP]$, $P = [\max(F_0^2,0)+2(F_c)^2]/3$, where $a = 0.0687$ and $b = 1.2398$ for **I**.

Karlsruhe, 76344 Eggenstein-Leopoldshafen, Germany (fax: +4 7247 808 666; e-mail: crysdata@fiz.karlsruhe.de) on quoting the depository number CSD418422.

Table 2
Atomic coordinates [$\times 10^4$] and equivalent isotropic displacement parameters [$Å^2 \times 10^3$] for $Mn_5(OH)_4(SO_3)_3 \cdot 2H_2O$, **I**

Atom	*x*	*y*	*z*	U_{eq}
Mn1	5533(1)	−509(1)	3585(1)	17(1)
Mn2	1920(1)	476(1)	1082(1)	17(1)
Mn3	5537(2)	−2500	1106(1)	15(1)
S1	2623(3)	2500	3901(2)	13(1)
S2	−1699(3)	2500	1146(2)	13(1)
S3	1517(3)	−2500	3137(2)	30(1)
O1	2430(8)	2500	2475(5)	19(1)
O2	3825(5)	1073(5)	4346(3)	22(1)
O3	−1016(5)	1068(5)	519(4)	22(1)
O4	−3728(7)	2500	683(5)	17(1)
O5	3540(7)	−2500	3329(6)	23(1)
O6	884(6)	−1113(7)	2395(5)	47(1)
O7	4646(5)	−196(5)	1593(3)	15(1)
O8	2330(7)	2500	−134(5)	14(1)
O9	6914(7)	−2500	3040(5)	16(1)
O10	8225(6)	699(6)	3828(4)	44(2)

U_{eq} is defined as the one-third of the orthogonalized tensor U_{ij}.

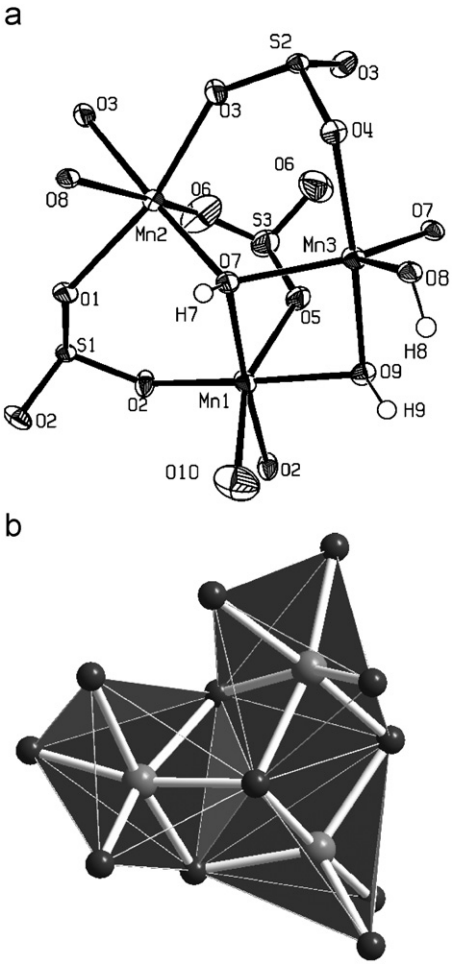

Fig. 1. (a) ORTEP diagram (at 50% probability) of **I** showing the atom-labeling scheme and (b) Mn_3O_{14} SBU polyhedra.

3. Results and discussion

The asymmetric unit of $Mn_5(OH)_4(SO_3)_3 \cdot 2H_2O$, **I**, as shown in Fig. 1(a), contains eleven and half non-hydrogen atoms with three crystallographically distinct Mn^{2+} ions with 2.5 occupancy, three SO_3^{2-} ions with half occupancy each, three hydroxyl ions with total of double occupancy and a water molecule. The Mn1 and Mn2 ions are in the 4*f* crystallographic position and have an octahedral coordination. The Mn3 ion is at the 2*e* crystallographic position with a trigonal bipyramidal coordination. The Mn1 ion is coordinated to three sulfite ions, two hydroxyl ions and a water molecule, while the Mn2 ion is coordinated to four sulfite ions and two hydroxyl ions. The Mn3 ion is coordinated to one sulfite ion and four hydroxyl ions. The hydroxyl, $O(7)H^-$, is μ_3_coordinated to the Mn1 and

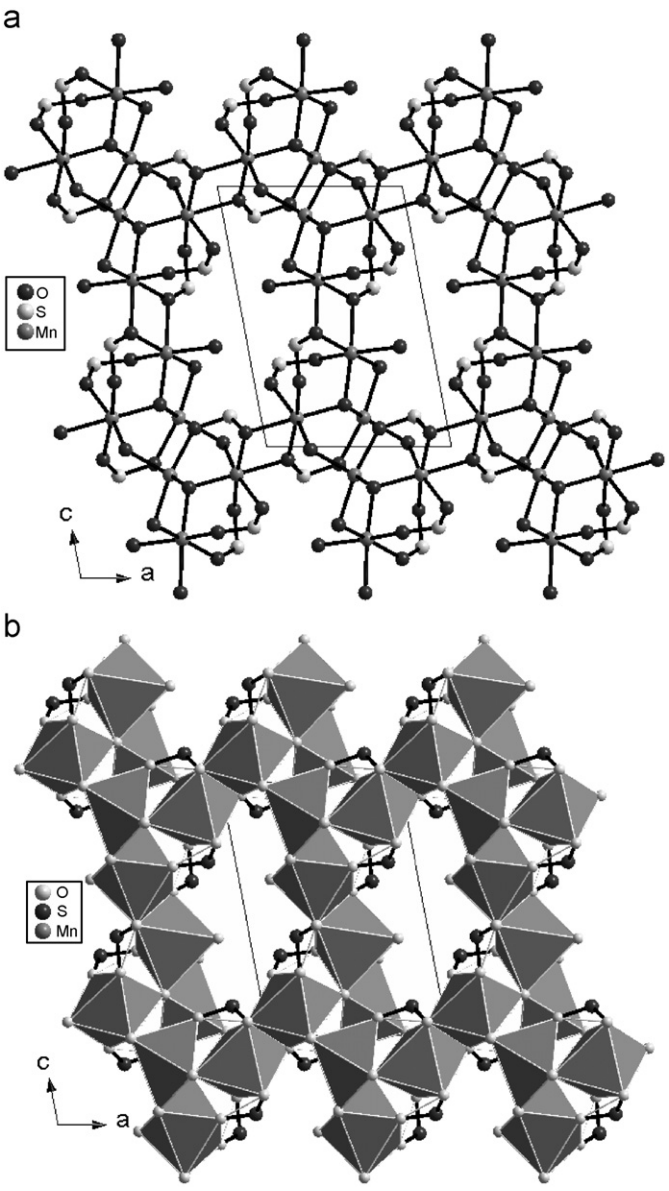

Fig. 2. (a) Ball and stick and (b) polyhedral representations of packing diagram, viewed along the *b*-axis of **I**.

Mn2 octahedra and the Mn3 trigonal bipyramid to form Mn_3O_{14} secondary building unit (SBU), as shown in Fig. 1(b). Each Mn_3O_{14} unit shares common edges and corners with the neighboring Mn_3O_{14} polyhedra along the three crystallographic axes, to form a three-dimensional structure with one-dimensional channels along the *b*-axis (Fig. 2). This arrangement gives rise to Mn–O–Mn linkages in three dimensions. The channel dimensions are 3.6 Å × 9.3 Å, but after subtracting the van der waals radii the dimensions reduce to 0.6 Å × 5.7 Å. The lone pair orbitals of the sulfite ions and the water molecules in **I**, point into the channel can be seen from Fig. 2. Specifically, the sulfite with a pyramidal geometry has the lone pair of electrons directed towards the fourth tetrahedral vertex. The Mn–O bond distances in **I** are in the range 2.088(5)–2.271(3) Å. The S–O bond distances are in the range of 1.454(5)–1.536(4) Å. The detailed list of bond distances in *I* is given in Table 3.

Variable temperature magnetic susceptibility data of **I** are shown in Fig. 3. From the high-temperature susceptibility data, we obtain a μ_{eff} 5.02 μ_B. The Curie–Weiss temperature is −13 K, indicating antiferromagnetic interactions between the Mn(II) centers. This magnetic behavior of *I* is similar to that reported in the case of manganese selenites [31].

TGA of **I** reveals that it is stable up to 180 °C. It undergoes a total weight loss of 39% in two steps in the 30–900 °C range. The powder X-ray diffraction pattern of the decomposed product corresponds to Mn_3O_4 (JCPDS file card 001-1127).

I exhibits interesting gas adsorption properties as shown in Fig. 4. The BET surface area of **I** calculated from the N_2 adsorption measurements is 2 m^2/g. Unlike N_2, O_2 and CO_2, adsorption of H_2 in **I** is substantial. Fig. 3 shows that the adsorption of H_2 at 77 K increases linearly with pressure and does not saturated upto 1 atm. The amount of H_2 absorbed at 77 K and 1 atm is 0.93 wt% (103 cc/g).

Table 3
Bond distances for $Mn_5(OH)_4(SO_3)_3 \cdot 2H_2O$, **I**

Moiety	Distances (Å)	Moiety	Distances (Å)
Mn1–9	2.127(3)	Mn3–O8 #3	2.088(5)
Mn1–O2	2.133(4)	Mn3–O4 #2	2.158(5)
Mn1–O7	2.157(4)	Mn3–O9	2.162(5)
Mn1–O5	2.247(4)	Mn3–O7	2.164(4)
Mn1–O10	2.253(5)	Mn3–O7 #4	2.164(4)
Mn1–O2 #1	2.259(4)	S1–O1	1.527(6)
Mn2–O7	2.115(4)	S1–O2	1.536(4)
Mn2–O3 #2	2.181(4)	S1–O2 #5	1.536(4)
Mn2–O6	2.208(5)	S2–O4	1.526(6)
Mn2–O8	2.221(3)	S2–O3	1.528(4)
Mn2–O3	2.251(4)	S2–O3 #5	1.528(4)
Mn2–O1	2.271(3)	S3–O6	1.454(5)
O7–H7	0.897(11)	S3–O6 #4	1.454(5)
O8–H8	0.899(11)	S3–O5	1.508(6)
O9–H9	0.899(11)		

Symmetry transformations used to generate equivalent atoms: #1 $-x+1, -y, -z+1$ #2 $-x, -y, -z$ #3 $-x+1, -y, -z$ #4 $x, -y-1/2, z$ #5 $x, -y+1/2, z$.

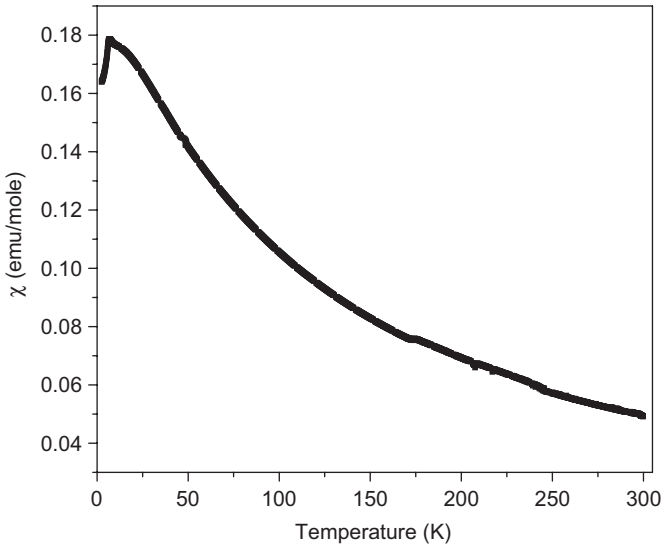

Fig. 3. Temperature variation of magnetic susceptibility of **I** (5000 Oe).

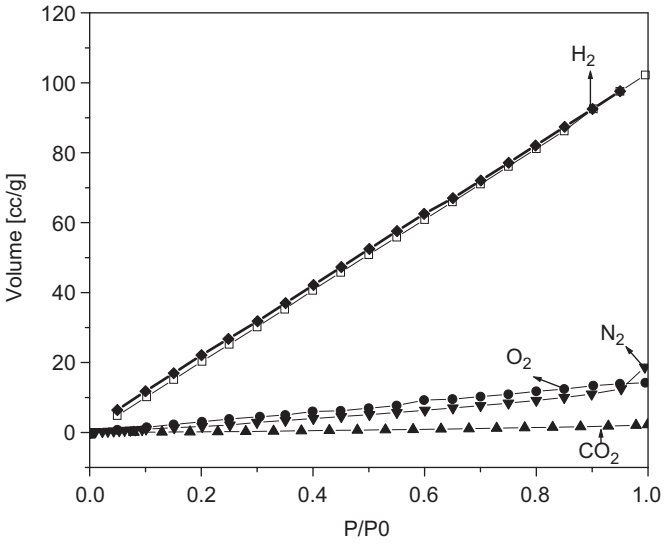

Fig. 4. Gas sorption isotherms of **I** at 77 K for H_2, N_2 and O_2 and for CO_2 at 195 K (1 atm). In the case of H_2, both adsorption (filled squares) and desorption (open squares) data are given.

This value is comparable to that of the nanoporous nickel (II) phosphate [12] and γ-zirconium phosphate [13]. In view of the good H_2 adsorption characteristics of **I**, we have carried out H_2 adsorption experiments at high pressures. In Fig. 5(a), we show the results of H_2 adsorption of **I**, at 300 K against different pressures. The wt% of H_2 adsorption reaches 2.1 at 134 bar and 300 K. In Figs. 5(b) and (c), we show the plots of pressure corresponding to the H_2 adsorbed against time at 300 and 77 K, respectively. While the amount of H_2 absorbed at 300 K and 134 bar is 2.1 wt%, that at 77 K and 17 bar is 1.3 wt%. These values of H_2 uptake are comparable with those of zeolites and zeolite-like compounds [32,33], most of which show H_2 adsorption of 1–2 wt% in the 77–300 K range and 1 atm. The number of gas molecules adsorbed per formula unit of

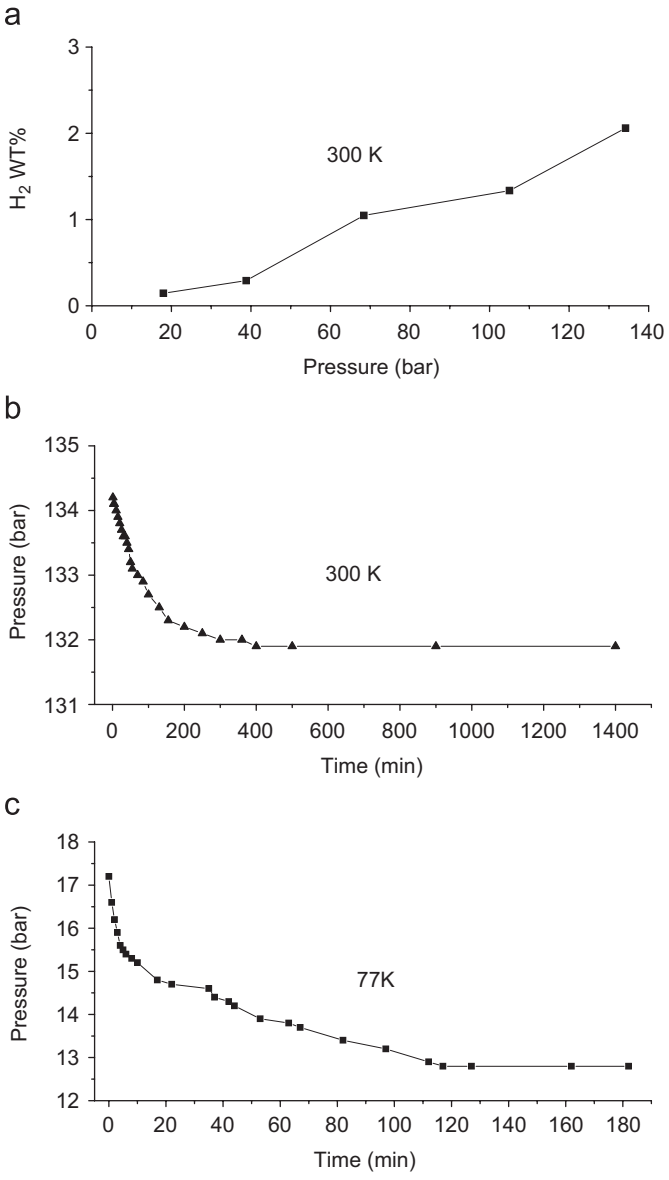

Fig. 5. (a) Plot of pressure versus time for **I** at 77 K and 17 bar. (b) Plot of pressure versus time for **I**, at 300 K and 134 bar. (c) Amount of hydrogen adsorbed in wt% at 300 K at different pressures.

I at 77 K (for CO_2 195 K) and 1 atm are 3, 0.5, 0.4 and 0.06 for H_2, N_2, O_2 and CO_2 gases, respectively. The selective sorption of the H_2 gas may be attributed to the small channel aperture in **I**, which can discriminate H_2 with a small kinetic diameter (2.8 Å) from the other gases with larger kinetic diameters. It is possible that there is weak interaction between H_2 and the metal atoms in **I**. It should be noted that in an ideal H_2 storage medium, the interaction between H_2 and the adsorption site should be some where between that in physisorption and chemisorption.

4. Conclusions

In conclusion, a manganese sulfite of the composition, $Mn_5(OH)_4(SO_3)_3 \cdot 2H_2O$, **I**, obtained by hydrothermal synthesis exhibits significant hydrogen uptake. The uptake of hydrogen is 0.93 wt% at 77 K and 1 atm, and reaches 2.1 wt% at 300 K and 134 bar. The compound is also interesting in that it contains Mn–O–Mn bonds in all the three dimensions.

References

[1] W. Breck, Zeolite Molecular Sieves, Wiley, New York, 1974.
[2] W.M. Meier, D.H. Oslen, C. Baerlocher, Atlas of Zeolite Structure Types, Elsevier, London, 1996.
[3] A.K. Cheetham, G. Férey, T. Loiseau, Angew. Chem. Int. Ed. 38 (1999) 3268.
[4] C.N.R. Rao, J.N. Behra, M. Dan, Chem. Soc. Rev. 35 (2006) 375.
[5] C.N.R. Rao, S. Natarajan, R. Vaidhyanathan, Angew. Chem. Int. Ed. 43 (2004) 1466.
[6] N.C. Ocwig, O. D-Friedrichs, M. O'Keefe, O.M. Yaghi, Acc. Chem. Res. 38 (2005) 176.
[7] P.M. Forster, A.K. Cheetham, Top Catal. 24 (2003) 79.
[8] G. Férey, C. M-Draznieks, C. Serre, F. Millange, J. Dutour, S. Surblé, I. Margiolaki, Science 309 (2005) 2040.
[9] R. Kitaura, K. Fujimoto, S. Noro, M. Kono, S. Kitagawa, Angew. Chem. Int. Ed. 41 (2002) 133.
[10] X. Zhao, B. Xiao, A.J. Fletcher, K.M. Thomas, D. Bradshaw, M.J. Rosseinsky, Science 306 (2004) 1012.
[11] A.K. Cheetham, C.N.R. Rao, Chem. Commun. (2006) 4780.
[12] P.M. Forster, J. Eckert, J.-S. Chang, S.-E. Park, G. Férey, A.K. Cheetham, J. Am. Chem. Soc. 125 (2003) 1309.
[13] E. Brnesto, H.M.H. Alhendawi, Angew. Chem. Int. Ed. 45 (2006) 6918.
[14] D.N. Dybtsev, H. Chun, S.H. Yoon, D. Kim, K. Kim, J. Am. Chem. Soc. 126 (2004) 32.
[15] A.C. Dillon, K.M. Jones, T.A. Bekkedahl, C.H. Kiang, D.S. Bethune, M.J. Heben, Nature 386 (1997) 377.
[16] C. Liu, Y.Y. Fan, M. Liu, H. Cong, H.M. Chen, M.S. Dresselhaus, Science 286 (1999) 1127.
[17] N.L. Rosi, J. Eckert, M. Eddaoudi, D.T. Vodak, J. Kim, M. O'Keefe, O.M. Yaghi, Science 300 (2003) 1127.
[18] A.M. Seayad, D.M. Antonelli, Adv. Mater. 16 (2004) 765.
[19] L.J. Florusse, C.J. Peters, J. Schoonman, K.C. Hester, C.A. Koh, S.F. Dec, K.N. Marsh, E.D. Sloan, Science 306 (2004) 469.
[20] S.M. Kuznicki, V.A. Bell, S. Nair, H.W. Hillhouse, R.M. Jacubinas, C.M. Braunbarth, B.H. Toby, M. Tsapatsis, Nature 412 (2001) 720.
[21] L. Pan, K.M. Adams, H.E. Hernandez, X. Wang, C. Zheng, Y. Hattori, K. Kaneko, J. Am. Chem. Soc. 125 (2003) 3062.
[22] K.P. Rao, C.N.R. Rao, Inorg. Chem. 46 (2007) 2511.
[23] K. Nakamoto, Infrared and Raman Spectra of Inorganic and Coordination Compounds, Wiley, New York, 1978.
[24] S. Barbara, Infrared Spectroscopy: Fundamentals and Applications, Wiley, New York, 2004.
[25] G. Gundiah, A. Govindaraj, N. Rajalakshmi, K.S. Dhathathreyan, C.N.R. Rao, J. Mater. Chem. 13 (2003) 209.
[26] K.S.W. Sing, D.H. Everett, R.A.W. Haul, L. Moscou, R.A. Pierotti, J. Rouquerol, T. Siemieniewska, Pure Appl. Chem. 57 (1985) 603.
[27] G.M. Sheldrick, SADABS: Siemens Area Detector Absorption Correction Program, University of Gottingen, Gottingen, Germany, 1994.
[28] L.J. Farrugia, J. Appl. Crystallogr. 32 (1999) 837.
[29] W.T. Pennington, DIAMOND Visual Crystal Structure Information System, J. Appl. Crystallogr. 32 (1999) 1029.
[30] L.J. Farrugia, ORTEP, J. Appl. Crystallogr. 30 (1997) 565.
[31] A. Larranaga, J.L. Mesa, J.L. Pizarro, R. Olazcuaga, M.I. Arriotua, T. Rojo, J. Chem. Soc. Dalton Trans. (2002) 3447.
[32] A. Zecchina, S. Bordiga, J.G. Vitillo, G. Ricchiardi, C. Lamberti, G. Spoto, M. Bjorgen, K.P. Lillerud, J. Am. Chem. Soc. 127 (2005) 6361.
[33] Y. Li, R.T. Yang, J. Phys. Chem. B 110 (2006) 17175.